Artificial Organs

Thoughts and Progress

Novel Application for Electrochemotherapy: Immersion of Nasal Cavity in Dog

*Daniela O.H. Suzuki, *José A. Berkenbrock, †Krishna D. de Oliveira, †Jennifer O. Freytag, and †Marcelo M.M. Rangel

*Institute of Biomedical Engineering, Federal University of Santa Catarina (UFSC), Florianópolis-SC; and †Oncology Veterinary, VetCâncer, São Paulo-SP, Brazil

Abstract: Electrochemotherapy is a new modality of local cancer treatment that increases the delivery of chemotherapy drugs into tumor cells by applying intense electric fields. This novel electrochemotherapy application was applied as an adjuvant to surgery and eliminated intranasal tumors in dog. The treatment challenges are the surgery limitations due to anatomy and residual tumor in the bone cavity. Most of the tumoral mass on nasal cavity was surgically removed. The internal nasal cavity was immersed in liquid and bleomycin before applying electric field. The solution was necessary to increase the superficial contact between plate electrodes and residual tumor. The numerical study demonstrated electrochemotherapy efficiency in different clinical situations. The proximity between electrodes and bone (<3 mm) and bone irregularities affect the electric field distribution on tumoral tissue. The tumoral tissue around bone protuberances tends to be eliminated. Electrochemotherapy with plate electrodes inside the cavity might not be effective. Different values of electric conductivity solution were studied; the ideal value was 0.5 S/m. The numerical and experimental results confirm the successful application of electrochemotherapy on dog nasal cavity. **Key Words:** Transmissible venereal tumor—Electric conductivity—Nasal tumor—Electric field—Electrochemotherapy.

Electrochemotherapy is a local cancer treatment; electric fields are applied to facilitate the passage of chemotherapic drugs into tumor cells. The treatment basis is the electroporation and electropermeabilization of cellular membrane (1–4). After the applied electric field exceeds a threshold value, the membrane permeability increases, permitting entrance of molecules, DNA, and drugs into cells. Nowadays, the theory of structural reorientation of phospholipid membranes and aqueous pore formation is confirmed by molecular dynamics simulation (1,5). Electric field strength, pulse duration, cell dimensions, electrical tissue anisotropy, number of pulses, pulse repetition frequency, and external conductivity may affect the electroporation (6–10).

The macroscopic effect of electroporation produces an increase in tissue electric conductivity and, consequently, alteration of local electric field distribution. The mathematical models for studying electrochemotherapy may present tissue electric conductivity dependent on electric fields (6,11–13). The clinical models consider a sufficiently high electric field needed for reversible electroporation and lower than irreversible electroporation for effective treatment. All tumor tissue needs to be electropermeabilized.

The Standard Operation Procedure (SOP) for electrochemotherapy describes the treatment of cutaneous and subcutaneous tumors (14). However, electrochemotherapy research presents indications of internal organs treatment, bone metastasis, novel electrodes, and head and neck cancer (3,15–17).

Tumors of the nasal cavity and paranasal sinuses (sinonasal tumors) in dogs account for 1% of all neoplasias. Sinonasal tumors usually occur in older dogs, with the average age at diagnosis between 10 and 15 years (18). Approximately 2/3 are carcinomas and 1/3 are sarcomas of all sinonasal tumors (19).

The purpose of this study was to demonstrate electrochemotherapy effectiveness on nasal cavity immersed in solution. The difficulties of this treatment include the anatomy and elimination of residual tumor after conservative surgery. The bone proximity (cavities and protuberances) and the electrical conductivity of solution on the tissues electric field distribution are investigated.

MATERIALS AND METHODS

In vivo electrochemotherapy

The case was the extension to the frontal sinus until palatine bone of a canine transmissible venereal tumor (CTVT), also called Sticker's sarcoma, in an 11-year-old poodle, 17 kg (Fig. 1). Before the electrochemotherapy, six sessions of vincristine

doi: 10.1111/aor.12858

Received June 2016; revised July 2016.

Address correspondence and reprint requests to Dr. Daniela O.H. Suzuki, Institute of Biomedical Engineering, Federal University of Santa Catarina (UFSC), CEP 88040-900, Florianópolis-SC, Brazil. E-mail: suzuki@eel.ufsc.br

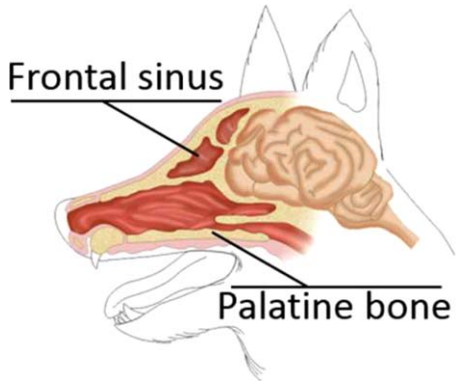

FIG. 1. Schematic representation of nasal cavity anatomy. The tumor was in the frontal sinus until the palatine bone. Inside the cavity the bones were irregular and did not allow total surgical elimination of the tumor. A solution with bleomycin filled the nasal cavity before applications of electric pulses and the residual tumor was eliminated. [Color figure can be viewed at wileyonlinelibrary.com.]

(0.7 mg/m^2) and two sessions of doxorubicin (30 mg/m^2) were administered. The animal showed disease progression. The clinical stage of the disease was based on advancement and clinical presentation of the disease. The electrochemotherapy treatments were administered after animal anesthesia and the tumoral mass was surgically removed (debulking surgery). The bone involvement was evident during the surgical procedure. There was no frontal bone, proximal and middle one-third nasal bone, and turbinate-ethmoid nasal bone. After the surgery, a vestige of tumor remained in the nasal cavities. The anatomic irregularity inside the cranial bone and the restrictve access to some surgical procedures produce this electrochemotherapy application. The intratumoral or intravenous injection of bleomycin was not viable. There were small soft tissues and the lesion area was extensive. The nasal cavity was immersed in a solution of bleomycin (1500 UI) and 30 mL 0.9% NaCl before the application of electric pulses. The bleomycin concentration was calculated based on blood volume for intravenous application (2), and blood volume was based on the dog's weight. The concentration of bleomycin in solution was about 10 times the bleomycin concentration in blood volume with intravenous injection (50 UI/mL). The bleomycin concentration was used to obtain a high enough concentration of the drug around the tumor. Eight electric pulses of 400 V/cm, 100 μs, and 10 Hz were generated with a BTX ECM 830 (Harvard Apparatus, Holliston, MA, USA), and were delivered in single session using two parallel, stainless-steel plate electrodes of 1 × 1 cm^2. After the treatment, the patient was clinically monitored for 1 year; there was no cancer recurrence. No antineoplasic drugs were given post-

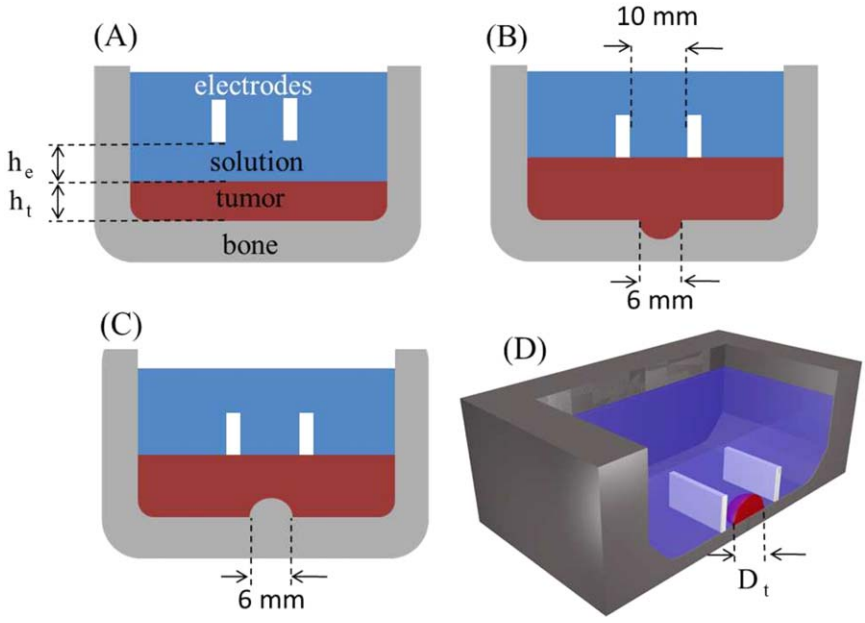

FIG. 2. The 3D numerical models for studying the electrical field distribution on a tumor immersed in conductive solution. The solution conductivity is 1.8 S/m. The schematic models represent the cutting plane of the nasal cavity. (A) Tumor plane surface covers the bone. h_t is the tumor thickness and h_e is the distance between electrodes and tumor. (B) Cavity in bone (6 mm) filled with tumor. (C) Bone protuberance. (D) Diameter of spherical tumor, D_t, immersed in solution. [Color figure can be viewed at wileyonlinelibrary.com.]

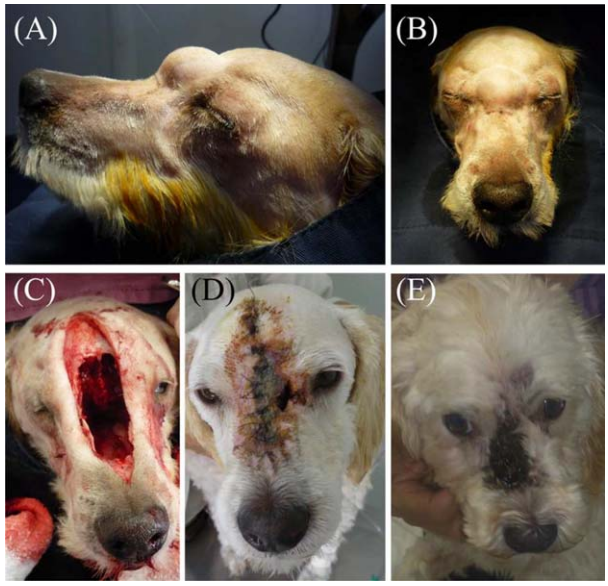

FIG. 3. Electrochemotherapy treatment of nasal tumor. (A) and (B) Facial deformation resulting from a nasal carcinoma (TVT). (C) Cranial opening applied with the solution and electrochemotherapy during the procedure. (D) Ninety-three days after the electrochemotherapy. (E) After 6 months, the patient was clinically monitored and there was no cancer recurrence. [Color figure can be viewed at wileyonlinelibrary.com.]

treatment. The experiments were performed in agreement with the recommendations of the ethical committee.

NUMERICAL MODELING

Finite element models were created using COMSOL Multiphysics 5.0 (Stockholm, Sweden) to demonstrate the electric field distributions on biological tissue. The resultant mesh was refined until the difference in numerical solution was less than 0.5%. The mesh of the models varied between 86,548 and 398,288 elements.

The electric field distribution models were calculated using the steady current module. Supposing that the electric current density J in the tissue is divergence-free, the solved equation is the Poisson's equation:

$$-\nabla \cdot (\sigma \nabla V) = 0, \quad (1)$$

where σ is the tissue conductivity (S/m) and V is the electric potential (V).

The boundary conditions were all insulating on the external surfaces (Neumann's boundary condition). The contact between plate electrode and tissue was modeled as Dirichlet's boundary condition.

The simulations have been performed assuming that electroporation increases the tumoral tissue conductivity (20). The tumor conductivity dependence on electric field is $\sigma(E) = 0.30 + 0.45\ (1 + \text{fe}) - 1$, $\text{fe} = 10\ \exp[0.20(60 - E)]$ (21). E is the local electric field (kV/m). The bone conductivity is 13 mS/m (22). The solution of 0.9% NaCl and bleomycin is 1.8 S/m (Hanna Instruments, Woonsocket, RI, USA).

In results, the values of E are displayed from reversible electric field $E_{\text{rev}} = 35$ kV/m to irreversible electric field $E_{\text{irrev}} = 80$ kV/m. The black color represents $E < E_{\text{rev}}$, no effect; gray color, $E_{\text{rev}} < E < E_{\text{irrev}}$, effective electrochemotherapy treatment; white color, $E > E_{\text{irrev}}$, irreversible electroporation.

Figure 2 presents the four models representing different parallel plate electrodes, conductivity mediums, and bone formations (plane, cavity, and protuberance). Distance between plates is 10 mm. The simulations are performed using 3D models. The first model describes two situations

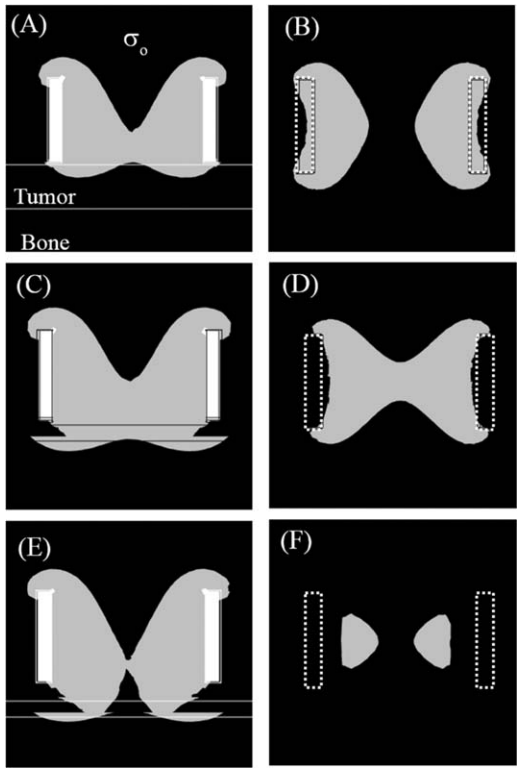

FIG. 4. Electric field distribution of 40 kV/m applied between electrode distance of 10 mm. The bone is covered by a tumor immersed in solution of $\sigma_0 = 1.8$ S/m. The left column shows a lateral cross section (perpendicular to tumor, skin, and electrode plate) and the right column shows a top cross section at 0.5 mm from tumor superficies. The dotted line is the electrode position. (A) and (B) Tumor height is 3 mm. (C) and (D) h_t is 1 mm. (E) and (F) h_t is 1 mm; the electrodes are not in tumor contact ($h_e = 1$ mm).

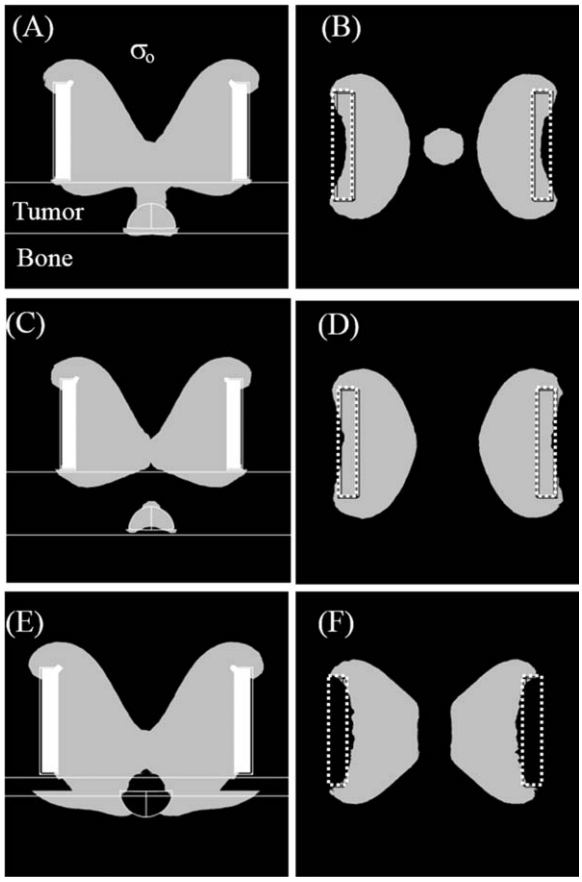

FIG. 5. Electric field distribution of tumor and bone model. The bone presents spheroidal cavity and protuberance covered by a tumor. The solution $\sigma_0 = 1.8$ S/m fills the external medium. The applied electric field is 40 kV/m; the distance between electrodes is 10 mm. The dotted line is the electrode position. The diameters of bone cavity and protuberance are 3 mm. (A) and (B) h_t is 3 mm. (C) and (D) h_t is 4 mm. (E) and (F) h_t is 1 mm.

considering the bone does not present imperfections. The electrodes' contact with the tumor tissue and thickness variation were validated. The second model and third model are used to analyze the bone effect on electrical field distributions. Figure 2D presents a half spherical tumor of D_t diameter. The variation in external conductivity was studied to improve the application.

The 3D model simulation was run on a personal computer (Intel Core i7, 2 GHz CPU, 8 GB RAM) with Windows 8.1 (×64, Microsoft, Inc., Redmond, WA, USA) operating system.

RESULTS

Figures 3A–D show the facial deformation caused by a Sticker's sarcoma from frontal sinus until palatine bone (Fig. 1). Figure 3C presents a surgical opening to access the internal nasal cavity. The great part of tumor mass was removed before the electrochemotherapy application. Figure 3D shows the dog 93 days after the treatment. The patient was monitored clinically for 6 months and did not present tumor recurrence, as shown by Fig. 3E.

Figure 4 shows simulation results when tumor covers the bone and the external medium is immersed in solution containing bleomycin ($\sigma_0 = 1.8$ S/m). Electric field distributions are presented for three situations: A and B, the tumor height is 3 mm; C and D, the tumor height is 1 mm; and E and F, there is no contact between tumor and electrodes.

The tumor area between electrodes was not eliminated by local electric field distributions as shown by Fig. 4A,B. The electric field covered tumor area between electrodes with bone proximity (Fig. 4C,D). The electrodes were not in contact with the tumor in Fig. 4E,F. However, electric field distribution presented distortion and tumor elimination caused by bone and conductivity solution.

Figure 5 presents the influence of bone protuberance and cavity on electric field distribution. Protuberances and cavity produce distorted electric field distribution on tumoral tissue.

It can be observed in Fig. 6 that the treatment efficiency is independent of tumor diameter. However, the contact surface between electrode and tumor provides unpermeabilized tissues, as shown

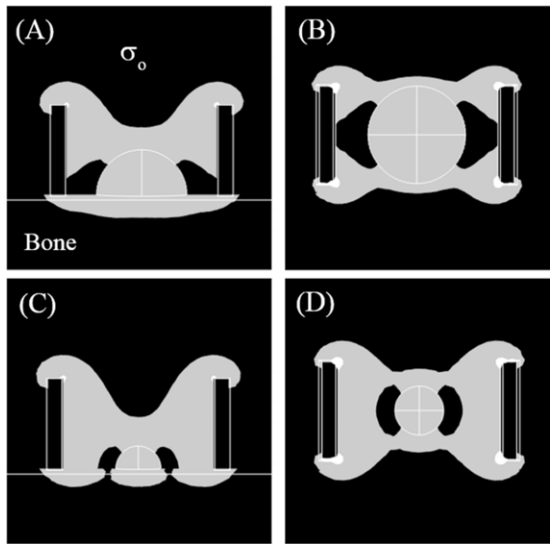

FIG. 6. Electric field distributions on different spheroidal tumor diameters. The electrode distance is 10 mm. The applied electric field is 40 kV/m and $\sigma_0 = 1.8$ S/m. (A) and (B) $D_t = 6$ mm. (C) and (D) $D_t = 3$ mm.

in Fig. 7A–D. Figure 7A,B presents a possible problem with solution of 1.8 S/m. The reduction of electric conductivity for 1 S/m is insufficient to eliminate the tumor. The medium conductivity of 0.5 S/m produced better electric field distribution; this surrounding conductivity eliminated all tumors (Fig. 7E,F).

Figure 8 shows the simulated electric field magnitude distributions for different medium conductivities ranging from 0.05 to 0.5 S/m, without contact between electrode and tumor. Electric field distribution in Figs. 8A,B did not cover all the tumor. When Figs. 8C,D were simulated with solution of 0.25 S/m, the tumor area eliminated by electrochemotherapy increased. The solution of 0.5 S/m presented completed elimination of tumor as shown by Fig. 8E,F.

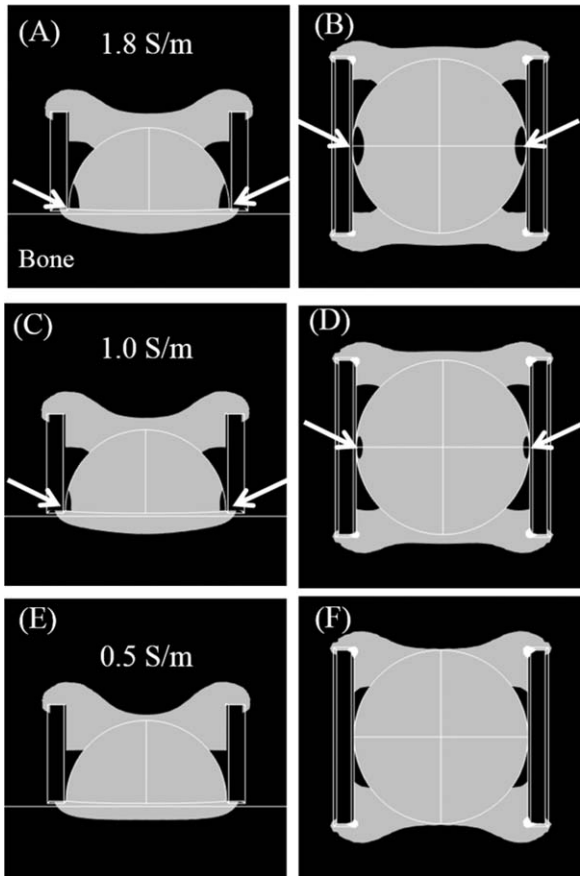

FIG. 7. Electric field distributions on spheroidal tumor diameters, $D_t = 10$ mm, with different solution conductivities. White arrows indicate where the electric field does not eliminate the tumor. The applied electric field is 40 kV/m and the electrode distance is 10 mm. (A) and (B) 1.8 S/m. (C) and (D) 1 S/m. (E) and (F) 0.5 S/m.

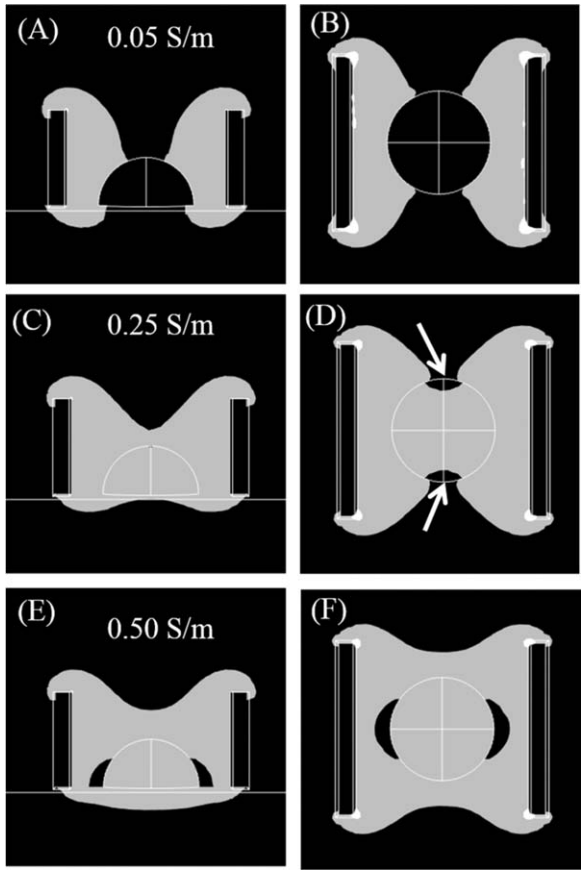

FIG. 8. Electric field distributions on spheroidal tumor diameters, $D_t = 6$ mm, with different solution conductivities. The applied electric field is 40 kV/m and the electrode distance is 10 mm. (A) and (B) 0.05 S/m. (C) and (D) 0.25 S/m; white arrows indicate where the electric field does not eliminate the tumor. (E) and (F) 0.5 S/m.

DISCUSSION

Most patients with tumor of the nasal cavity have advanced-stage disease before signs and symptoms develop. The tumor treatment of this intricate anatomy is challenging, particularly in patients with locally advanced disease. The primary treatment approach for patients with these tumors is radical surgery (rhinothomy) followed by radiotherapy or chemotherapy; some benefits were obtained with postoperative chemoradiotherapy (23). However, over 80% of the tumors are malignant (19), and the poor long-term prognosis may be caused by residual tumor in bone cavity and protuberances. This novel application of electrochemotherapy eliminated the residual tumor tissue from conservative surgery and dispensed with postoperative treatment, as shown in Fig. 3.

In this treatment, the electric field applied is weaker than in electrochemotherapy of cutaneous

and subcutaneous tumors (1300 V/cm) (2). 400 V/cm is a strong electric field but it does not exceed the electric current limit of equipment. Treatment efficiency occurs because the treatment is applied on tumoral tissue (without low tissue conductivity, like stratum corneum), bone proximity, and ionic solution (Figs. 4, 6, and 8).

Works on subcutaneous and cutaneous tumors consider the E_{rev} for electrochemotherapy from 400 V/cm (24,25) to 866 V/cm (11) and the E_{irrev} from 900 V/cm (26) to 1733 V/cm (11). Pavšelj et al. (25) demonstrated that an electric field about 300 V/cm increases the current measured on melanoma B16 and LPB sarcoma. In vitro permeabilization of B16F10 cells was detected only for electric field values higher than 300 V/cm (27). Mossop et al. (17) verified with experiments on 4T1 and B16F10 tumors that the tissue resistivity decreases with an electric field over 300 V/cm. Electrochemotherapy of intracranial tumor proposed $E_{rev} = 350$ V/cm as a threshold value (28). In this work, the electric field displayed was from reversible $E_{rev} = 350$ V/cm to the irreversible electroporation threshold value $E_{irrev} = 800$ V/cm. These values of electric fields ensure a safe treatment of nasal cavity tumors.

The bone affects the electric field distribution on tumor tissue when the distance between electrodes and bones is less than 3 mm, as shown in Fig. 4C–E. The bone attracts the electric field and increases the eliminated tumoral area. This effect is produced because the bone conductivity is smaller than biological tissue conductivities (e.g., tumor, dermis, and muscle). The electric current deviates from bones; it is concentric on biological tissues around bones. The current density in these places produces high local electric field. The protuberances increase the tumoral area eliminated by the treatment (Fig. 5A–D). Figure 5E shows that inside the bone cavity the tumor is not affected by the electric field.

The high electric conductivity of solution (1.8 S/m) produces homogeneous electric field distribution inside the spherical tumor (Fig. 6A–D). Ivorra et al. (11) covered the tumor with gel to improve the electric field distribution inside the tumor. Electric field distribution on cutaneous tumor with plate electrodes is not homogeneous; it depends on the electrode contacts (24). The contact is important when the external medium around the tumor and the electrode is air (24). It becomes a problem when the tumor is immersed in high electric conductivity (Fig. 7A–D). Without electrode contact, the electric field is homogeneous inside the tumor and electrochemotherapy is effective, as shown in Fig. 6A–D. We do not recommend electrode contact with this solution.

The ideal external solution to electrochemotherapy on bone cavity has electrical conductivity of 0.5 S/m (Figs. 7E,F and 8E,F). This conductivity value agrees with the gel conductivity proposed by Ivorra et al. (11) and Suzuki et al. (29). We suggest a 1/4 dilution of 0.9% sodium chloride and bleomycin (1500 UI). This electric conductivity reduction improves tumor elimination and decreases the medium current of electroporator power supply.

CONCLUSION

The results of this work demonstrated that this novel electrochemotherapy application may be effective on tumor elimination into the nasal cavity. Our findings demonstrated that bone proximity with electrode (<3 mm) is an important factor to be considered in electrochemotherapy applications. The liquid conductivity for this application was 0.9% NaCl, 1.8 S/m. An improvement to this application can be made by reducing the electrical conductivity of solution to 1/4.

Acknowledgment: This study was supported by CNPq (National Council for Scientific and Technological Development).

Conflict of Interest: The authors declare no conflict of interest.

REFERENCES

1. Cemazar M, Kotnik T, Serša G, Miklavčič D. Electroporation for electrochemotherapy and gene therapy. In: Marko MS, ed. *Electromagnetic Fields in Biology and Medicine*. Boca Raton: CRC Press, 2015:395–413.
2. Marty M, Serša G, Garbay JR, et al. Electrochemotherapy—an easy, highly effective and safe treatment of cutaneous and subcutaneous metastases: results of ESOPE (European Standard Operating Procedures of Electrochemotherapy) study. *Eur J Cancer Suppl* 2006;4:3–13.
3. Miklavčič D, Mali B, Kos B, Heller R, Serša G. Electrochemotherapy: from the drawing board into medical practice. *Biomed Eng Online* 2014;13:29.
4. Spugnini EP, Citro G, Baldi A. Adjuvant electrochemotherapy in veterinary patients: a model for the planning of future therapies in humans. *J Exp Clin Cancer Res* 2009;28:114.
5. Delemotte L, Tarek M. Molecular dynamics simulations of lipid membrane electroporation. *J Membr Biol* 2012;245:531–43.
6. Čorović S, Županič A, Kranjc S, Al-Sakere B, Leroy-Willig A, Mir LM, et al. The influence of skeletal muscle anisotropy on electroporation: in vivo study and numerical modeling. *Med Biol Eng Comput* 2010;48:637–48.
7. Li J, Tan W, Yu M, Lin H. The effect of extracellular conductivity on electroporation-mediated molecular delivery. *Biochim Biophys Acta - Biomembr* 2013;1828:461–70.
8. Pucihar G, Mir L, Miklavčič D. The effect of pulse repetition frequency on the uptake into electropermeabilized cells

in vitro with possible applications in electrochemotherapy. *Bioelectrochemistry* 2002;57:167–72.
9. Suárez C, Soba A, Maglietti F, Olaiz N, Marshall G. The role of additional pulses in electropermeabilization protocols. *PLoS ONE* 2014;9:e113413.
10. Suzuki DOH, Ramos A, Ribeiro MCM, et al. Theoretical and experimental analysis of electroporated membrane conductance in cell suspension. *IEEE Trans Biomed Eng* 2011;58:3310–8.
11. Ivorra A, Al-Sakere B, Rubinsky B, Mir LM. Use of conductive gels for electric field homogenization increases the antitumor efficacy of electroporation therapies. *Phys Med Biol* 2008;53:6605–18.
12. Miklavčič D, Serša G, Brecelj E, et al. Electrochemotherapy: technological advancements for efficient electroporation-based treatment of internal tumors. *Med Biol Eng Comput* 2012;50:1213–25.
13. Suzuki DOH, Anselmo J, de Oliveira KD, et al. Numerical model of dog mast cell tumor treated by electrochemotherapy. *Artif Organs* 2014;39:192–7.
14. Mir LM, Gehl J, Serša G, et al. Standard operating procedures of the electrochemotherapy: instructions for the use of bleomycin or cisplatin administered either systemically or locally and electric pulses delivered by the CliniporatorTM by means of invasive or non-invasive electrodes. *Eur J Cancer Suppl* 2006;4:14–25.
15. Campana LG, Cesari M, Dughiero F, et al. Electrical resistance of human soft tissue sarcomas: an ex vivo study on surgical specimens. *Med Biol Eng Comput* 2015;54:773–87.
16. Fini M, Salamanna F, Parrilli A, et al. Electrochemotherapy is effective in the treatment of rat bone metastases. *Clin Exp Metastasis* 2013;30:1033–45.
17. Mossop BJ, Barr RC, Henshaw JW, Zaharoff DA, Yuan F. Electric fields in tumors exposed to external voltage sources: implication for electric field-mediated drug and gene delivery. *Ann Biomed Eng* 2006;34:1564–72.
18. Wilson DW, Dungworth DL. Tumors of the respiratory tract. In: Meuten DJ, ed. *Tumors in Domestic Animals*. Iowa: Iowa State Press, 2002:365–73.
19. Elliot KM, Mayer MN. Radiation therapy for tumors of the nasal cavity and paranasal sinuses in dogs. *Can Vet J* 2009; 50:309–12.
20. Miklavčič D, Sel D, Cukjati D, Batiuskaite D, Slivnik T, Mir LM. Sequential finite element model of tissue electropermeabilisation. *IEEE Trans Biomed Eng* 2005;52:816–27.
21. Corovic S, Lackovic I, Sustaric P, Sustar T, Rodic T, Miklavcic D. Modeling of electric field distribution in tissues during electroporation. *Biomed Eng Online* 2013;12:1–16.
22. Gabriel S, Lau RW, Gabriel C. The dielectric properties of biological tissues: III. Parametric models for the dielectric spectrum of tissues. *Phys Med Biol* 1996;41:2271–93.
23. Wiegner EA, Daly ME, Murphy JD, et al. Intensity-modulated radiotherapy for tumors of the nasal cavity and paranasal sinuses: clinical outcomes and patterns of failure. *Int J Radiat Oncol Biol Phys* 2012;83:243–51.
24. Čorović S, Al-Sakere B, Haddad V, Miklavčič D, Mir LM. Importance of contact surface between electrodes and treated tissue in electrochemotherapy. *Technol Cancer Res Treat* 2008;7:393–400.
25. Pavselj N, Bregar Z, Cukjati D, Batiuskaite D, Mir LM, Miklavčič D. The course of tissue permeabilization studied on a mathematical model of a subcutaneous tumor in small animals. *IEEE Trans Biomed Eng* 2005;52:1373–81.
26. Čorović S, Zupanic A, Miklavčič D. Numerical modeling and optimization of electric field distribution in subcutaneous tumor treated with electrochemotherapy using needle electrodes. *IEEE Trans Plasma Sci* 2008;36:1665–72.
27. Paganin-Gioanni A, Bellard E, Couderc B, Teissié J, Golzio M. Tracking in vitro and in vivo siRNA electrotransfer in tumor cells. *J RNAi Gene Silencing* 2008;4:281–8.
28. Mahmood F, Gehl J. Optimizing clinical performance and geometrical robustness of a new electrode device for intracranial tumor electroporation. *Bioelectrochemistry* 2011;81: 10–6.
29. Suzuki DOH, Marques CMG, Rangel MMM. Conductive gel increases the small tumor treatment with electrochemotherapy using needle electrodes. *Artif Organs* 2015;40:705–11.